

BLOCCS: Block Sparse Canonical Correlation Analysis With Application To Interpretable Omics Integration

Omid Shams Solari,^{1*}, Rojin Safavi², James B. Brown¹

¹Statistics Department, University of California, Berkeley

²Department of Bio-Engineering, University of California, Santa Cruz

Abstract

We introduce *Block Sparse Canonical Correlation Analysis* which estimates multiple pairs of canonical directions (together a “block”) at once, resulting in significantly improved orthogonality of the sparse directions which, we demonstrate, translates to more interpretable solutions. Our approach builds on the sparse CCA method of (Solari, Brown, and Bickel 2019) in that we also express the bi-convex objective of our block formulation as a concave minimization problem over an orthogonal k -frame in a unit Euclidean ball, which in turn, due to concavity of the objective, is shrunk to a Stiefel manifold, which is optimized via gradient descent algorithm. Our simulations show that our method outperforms existing sCCA algorithms and implementations in terms of computational cost and stability, mainly due to the drastic shrinkage of our search space, and the correlation within and orthogonality between pairs of estimated canonical covariates. Finally, we apply our method, available as an R-package called *BLOCCS*, to multi-omic data on *Lung Squamous Cell Carcinoma(LUSC)* obtained via *The Cancer Genome Atlas*, and demonstrate its capability in capturing meaningful biological associations relevant to the hypothesis under study rather than spurious dominant variations.

1 Introduction

Multi-view¹ observations, i.e. observations of multiple random vectors or feature sets on matching individuals, are increasingly ubiquitous in data science, particularly. In molecular biology, multiple ”omics” layers are regularly collected – measurements that sample comprehensively from an underlying pool of molecules, such as a genome, or the set of all RNA transcripts, known as the transcriptome. For example, The Cancer Genome Atlas (TCGA) is a multi-omics molecular characterization of tumors across thousands of patients. In such studies, we are often interested in understanding how two or more omics layers, or views, are related to one another – e.g., how genotype relates to gene expression, revealing transcriptional regulatory relationships – for

a review see (Li, Wu, and Ngom 2016). This is very different from classical regression settings, where we have a one-dimensional response that we aim to model as a function of a vector of explanatory variables. As a result, new models are needed to enable the discovery of interpretable hypotheses regarding the association structures in multi-view settings, including multi-omics.

Canonical Correlation Analysis(CCA), (Hotelling 1935), is one set of such models whose objective is to find linear combinations of two sets of random variables such that they are maximally correlated. CCA is the most popular approach up to date in such settings which has been applied in almost all areas of science including: medicine (Monmonier and Finn 1973), policy (Hopkins 1969), physics (Wong, Fung, and Lau 1980), chemistry (Tu et al. 1989), and finance (Simmonson, Stowe, and Watson 1983). Several variants of CCA to incorporate non-linear combinations of covariates, e.g. Kernel CCA of (Lai and Fyfe 2000) and Deep CCA of (Andrew et al. 2013), have also been widely particularly popular in neuro-imaging (Blaschko et al. 2011), computer vision (Huang et al. 2010), and genetics (Chaudhary et al. 2018).

Despite various improvements in multi-view models, inference, interpretability and model selection is still a challenge, which is mainly owed to very high-dimensional multi-view observations that become increasingly common as high-throughput measurement systems advance. Variable selection via sparsity inducing norms is a popular approach to identifying interpretable association structures in such high-dimensional settings, which are particularly important since, from a biological perspective, it is likely that responses of interest arise from the action of genes functioning in pathways. In other words, for a particular outcome, such as disease-free survival in particular cancer, not all genes are relevant, or, to use the multi-view learning parlance, “active”. Hence, the derivation of sparse models from the analysis of multi-omics data is of intrinsic interest to biological data scientists.

While several sparse CCA methods are available, (Witten and Tibshirani 2009), (Parkhomenko, Tritchler, and Beyene 2009), (Waaijenborg, Verselewel de Witt Hamer, and Zwinderman 2008), (Chu D. 2013), their lack of stability and empirical consistency, and additionally their high computa-

*corresponding author: solari@berkeley.edu

Copyright © 2020, Association for the Advancement of Artificial Intelligence (www.aaai.org). All rights reserved.

¹Each dataset containing observations on random vectors is termed a *view* in this article.

tional cost, makes them unsuitable non-parametric hypothesis testing or hyperparameter tuning. (Solari, Brown, and Bickel 2019) introduce MuLe which is a set of approaches to solving sparse CCA problems using power iterations. They demonstrate superior stability and empirical consistency compared to other popular algorithms as well as significantly lower computational cost. One shortcoming however, which is common among all sparse CCA and sparse PCA approaches, is that none guarantee, or even heuristically enforce, orthogonality between estimated canonical directions. Here, our approach also relies on power iterations; however, we address the lack of orthogonality by estimating multiple canonical directions at once – adapting a block formulation for novel use in sparse CCA (Journée et al. 2010).

2 Notation

We denote scalar, vector, and matrix parameters by lower-case normal, lower-case bold, and upper-case bold letters, respectively, and random variables by upper-case normal letters. Hence, each view, i.e. the observation matrix on random vector $X_i(\omega) : \Omega \rightarrow \mathbb{R}^{p_i}$, is denoted by $\mathbf{X}_i \in \mathbb{R}^{n \times p_i}$, $i = 1, \dots, m$. n is used to indicate the sample size and p_i the dimensionality of the covariate space of each of m views. Canonical directions are denoted by $\mathbf{z}_i \in \mathcal{B}^{p_i}$, or $\mathbf{z}_i \in \mathcal{S}^{p_i}$, and $\mathbf{Z}_i \in \mathcal{S}_d^{p_i}$, where $\mathcal{B} = \{\mathbf{x} \in \mathbb{R} \mid \|\mathbf{x}\|_2 \leq 1\}$ and $\mathcal{S} = \{\mathbf{x} \in \mathbb{R} \mid \|\mathbf{x}\|_2 = 1\}$. $\mathcal{S}_d^p = \{\mathbf{Z} \in \mathbb{R}^{p \times d} \mid \mathbf{Z}^\top \mathbf{Z} = \mathbf{I}_d\}$ denotes a *Stiefel* manifold which is the space of orthonormal d -frames. $l_x(\mathbf{z}) : \mathbb{R}^p \rightarrow \mathbb{R}$ denotes any norm function, more specifically $l_{0/1}(\mathbf{z}) = \|\mathbf{z}\|_{0/1}$, and $\tau^{(i)}$ refers to the i – th non-zero element of the vector which is specifically used for the sparsity pattern vector. We also introduce *accessory variables* in Section 4.3 to term variables towards which we direct estimated canonical directions, neglecting their inferential role as covariates or dependent variables. We also use “program” to refer to “optimization programs”.

3 Background

Sub-space learning is perhaps the most popular concept in multi-view learning, and implies a *Latent Space* generative model, where each view, $X_i(\omega) : \mathcal{U} \rightarrow \mathcal{X}_i, i = 1, \dots, m$, is assumed to be a function of a common unobservable random vector, $U : \Omega \rightarrow \mathcal{U}$ in the latent space. The main objective in subspace learning is to estimate the inverse of these mappings within a functional family, $\mathcal{F}_i = \{F_i : \mathcal{X}_i \rightarrow \mathcal{U}\}$ assuming invertibility. At the sample level, this is interpreted as estimating $F_i(X_i)$ by $\mathbf{F}_i : \mathbb{R}^{n \times p_i} \rightarrow \mathcal{U}^n$ such that some similarity measure, $\mathcal{S} : \mathcal{U}^{n \times m} \rightarrow \mathbb{R}^d$ between these transformed observed views is maximized,

$$\mathbf{F}^* = \arg \max_{\substack{F_i \in \mathcal{F}_i \\ i \in \{1, \dots, m\}}} \mathcal{S}(F_1(X_1), \dots, F_m(X_m)) \quad (1)$$

Where $\mathbf{F} = (F_1, \dots, F_m)$. d is the number of dimensions in which similarity is maximized, which is of importance since here we are concerned with block algorithms where $d > 1$. In the rest of this section and most of Section 4 we assume that we observe only a pair of views, i.e. $m = 2$. Throughout this paper we also assume that $U : \Omega \rightarrow \mathbb{R}^k$, $X_i : \mathbb{R}^k \rightarrow \mathbb{R}^{p_i}$.

3.1 Canonical Correlation Analysis

If we assert the functional families \mathcal{F}_i to be a subset of the parametric family of linear functions $\mathcal{L} = \{l_i : \mathbb{R}^{p_i} \rightarrow \mathbb{R}^k, l_i(X_i) = \mathbf{z}_i X_i\}$, and the similarity criterion to be the Pearson correlation, we end up with the *Canonical Correlation Analysis* criterion. Assuming $E[X_1] = \mathbf{0}^{p_1}$ and $E[X_2] = \mathbf{0}^{p_2}$,

$$\begin{aligned} (\mathbf{z}_1^*, \mathbf{z}_2^*) &= \arg \max_{\mathbf{z}_1 \in \mathbb{R}^{p_1}, \mathbf{z}_2 \in \mathbb{R}^{p_2}} \rho(X_1 \mathbf{z}_1, X_2 \mathbf{z}_2) \\ &= \arg \max_{\mathbf{z}_1 \in \mathbb{R}^{p_1}, \mathbf{z}_2 \in \mathbb{R}^{p_2}} \frac{E[(X_1 \mathbf{z}_1)^\top (X_2 \mathbf{z}_2)]}{\sqrt{E[(X_1 \mathbf{z}_1)^2]^{1/2} E[(X_2 \mathbf{z}_2)^2]^{1/2}}} \end{aligned} \quad (2)$$

Since we almost always have access only to samples from X_1 and X_2 , we estimate Equation 2 using plug-in sample estimators for population terms.

$$(\mathbf{z}_1^*, \mathbf{z}_2^*) = \arg \max_{\mathbf{z}_1 \in \mathbb{R}^{p_1}, \mathbf{z}_2 \in \mathbb{R}^{p_2}} \frac{\mathbf{z}_1^\top \mathbf{X}_1^\top \mathbf{X}_2 \mathbf{z}_2}{\sqrt{\mathbf{z}_1^\top \mathbf{X}_1^\top \mathbf{X}_1 \mathbf{z}_1} \sqrt{\mathbf{z}_2^\top \mathbf{X}_2^\top \mathbf{X}_2 \mathbf{z}_2}} \quad (3)$$

\mathbf{z}_i are termed *Canonical Loading Vectors* and $\mathbf{X}_i \mathbf{z}_i$ are called the *Canonical Covariates*.

4 Block Reformulations of CCA Models

Generalizing Program 3 to $\mathbf{Z}_i \in \mathbb{R}^{p_i \times d}$,

$$(\mathbf{Z}_1^*, \mathbf{Z}_2^*) = \arg \max_{\substack{\mathbf{Z}_1 \in \mathbb{R}^{p_1 \times d}, \mathbf{Z}_2 \in \mathbb{R}^{p_2 \times d} \\ \mathbf{Z}_1^\top \mathbf{X}_1^\top \mathbf{X}_1 \mathbf{Z}_1 = \mathbf{Z}_2^\top \mathbf{X}_2^\top \mathbf{X}_2 \mathbf{Z}_2 = \mathbf{I}^d}} \text{tr}(\mathbf{Z}_1^\top \mathbf{X}_1^\top \mathbf{X}_2 \mathbf{Z}_2) \quad (4)$$

Here we reserve the term “*block formulation*” to discuss settings in which $d > 1$. As is customary in the regularized CCA literature[cite sandrine], here we also assume that $\mathbf{X}_i^\top \mathbf{X}_i = \mathbf{I}^{p_i}, i = 1, 2, \dots$, which enables us to rewrite Program 4 as,

$$(\mathbf{Z}_1^*, \mathbf{Z}_2^*) = \arg \max_{\substack{\mathbf{Z}_1 \in \mathcal{S}_d^{p_1} \\ \mathbf{Z}_2 \in \mathcal{S}_d^{p_2}}} \text{tr}(\mathbf{Z}_1^\top \mathbf{X}_1^\top \mathbf{X}_2 \mathbf{Z}_2) \quad (5)$$

Where \mathcal{S}_d^p is a *Stiefel Manifold*²

4.1 Regularized Block CCA

We analyze the following generalized formulation of the sparse block CCA problem in this section,

$$\begin{aligned} \phi_{l,d}(\gamma_1, \gamma_2) &:= \max_{\substack{\mathbf{Z}_1 \in \mathcal{S}_d^{p_1} \\ \mathbf{Z}_2 \in \mathcal{S}_d^{p_2}}} \text{tr}(\mathbf{Z}_1^\top \mathbf{C}_{12} \mathbf{Z}_2 \mathbf{N}) \\ &\quad - \sum_{j=1}^d \gamma_{1j} l(\mathbf{z}_{1j}) - \sum_{j=1}^d \gamma_{2j} l(\mathbf{z}_{2j}) \end{aligned} \quad (6)$$

$\gamma_i \in \mathbb{R}^d, \gamma_i \geq 0$ is the sparsity parameter vector for each view, and $\mathbf{N} = \text{diag}(\boldsymbol{\mu}), \boldsymbol{\mu} \in \mathbb{R}^+$, where d is the number

² $\mathcal{S}_m^p = \{\mathbf{M} \in \mathbb{R}^{p \times d} \mid \mathbf{M}^\top \mathbf{M} = \mathbf{I}\}$

of canonical covariates. $l(\mathbf{z}_{ij})$ is some norm of the $j - th$ column of the $i - th$ view, and \mathbf{C}_{12} is the sample covariance matrix.

Remark 1 In practice, distinct μ_i enforces the objective in Program 6 to have distinct maximizers (Journée et al. 2010).

l_1 -Regularization Here we consider Equation 6 with l_1 -regularization, and decouple the problem along multiple canonical directions resulting in the following program,

$$\begin{aligned} \phi_{l_1,d}(\gamma_1, \gamma_2) = \max_{\mathbf{Z}_1 \in \mathcal{S}_d^{p_1}} \sum_{j=1}^d \max_{\mathbf{z}_{2j} \in \mathcal{S}^{p_2}} & [\mu_j \mathbf{c}_i^\top \mathbf{z}_{1j} \mathbf{C}_{12} \mathbf{z}_{2j} - \gamma_{2j} \|\mathbf{z}_{2j}\|_1] \\ & - \sum_{j=1}^d \gamma_{1j} \|\mathbf{z}_{1j}\|_1 \end{aligned} \quad (7)$$

where \mathbf{z}_{ij} is the j -th column of the i -th dataset.

Theorem 2 Maximizers \mathbf{Z}_1^* and \mathbf{Z}_2^* of Program 7 are,

$$\mathbf{Z}_1^* = \arg \max_{\mathbf{Z}_1 \in \mathcal{S}_d^{p_1}} \sum_{j=1}^d \sum_{i=1}^{p_2} [\mu_j |\mathbf{c}_i^\top \mathbf{z}_{1j}| - \gamma_{2j}]_+^2 - \sum_{j=1}^d \gamma_{1j} \|\mathbf{z}_{1j}\|_1 \quad (8)$$

and,

$$[\mathbf{Z}_2]_{ij}^* = \frac{\operatorname{sgn}(\mathbf{c}_i^\top \mathbf{z}_{1j}) [\mu_j |\mathbf{c}_i^\top \mathbf{z}_{1j}| - \gamma_{2j}]_+}{\sqrt{\sum_{k=1}^{p_2} [\mu_j |\mathbf{c}_k^\top \mathbf{z}_{1j}| - \gamma_{2j}]_+^2}} \quad (9)$$

Equation 9 is utilized to derive the necessary and sufficient conditions under which z_{2ji}^* is active, i.e. inferring the sparsity pattern matrix, $\operatorname{supp}(\mathbf{Z})$, which is denoted her by $\mathbf{T}_2 \in \{0, 1\}^{p_2 \times d}$.

Corollary 3 $[\mathbf{T}_2]_{ij} = 0$, i.e. $z_{2ji}^* \in \operatorname{supp}(\mathbf{Z}_2^*)$, iff $|\mathbf{c}_i^\top \mathbf{z}_{1j}^*| \leq \gamma_{2j} / \mu_j$.

Theorem 2 enables us to infer the the sparsity pattern of either of the canonical directions due to the symmetry of the problem. Assuming we estimate \mathbf{T}_2 first, we shrink the sample covariance matrix to $[\mathbf{C}'_{12}]_{kl} = [\mathbf{C}_{12}]_{k\tau_{2j}^{(l)}}$ where $\tau_{2j}^{(l)}$ is the l -th non-zero element of the j -th column of \mathbf{T}_2 . We then use this reduced covariance matrix to estimate \mathbf{T}_1 . Having estimated the sparsity pattern matrices in the first stage, we estimate the active elements of the canonical direction matrices in the second stage by first shrinking the covariance matrix on both sides, resulting in $[\mathbf{C}_{12}^{(j)}]_{kl} = [\mathbf{C}_{12}]_{\tau_{1j}^{(k)}, \tau_{2j}^{(l)}}$, then estimating its active elements via an alternating algorithm introduced in 5.2.

Remark 4 According to Theorem 2, in order to infer the sparsity pattern matrices, we need to maximize Program 9. This program is non-convex; however we approximate it by ignoring the penalty term which turns it into the following concave minimization over the unit sphere,

$$\phi_{l_1,d}(\gamma_1, \gamma_2) = \max_{\mathbf{Z}_1 \in \mathcal{S}_d^{p_1}} \sum_{j=1}^d \left\{ \sum_{i=1}^{p_2} [\mu_j |\mathbf{c}_i^\top \mathbf{z}_{1j}| - \gamma_{2j}]_+^2 \right\} \quad (10)$$

which is solved using a simple gradient ascent algorithm. It is important to note that this approximation is justifiable. Our simulations demonstrate that this approximation does not affect the capability of our approach to uncover the support of our underlying generative model. Secondly, as we have mentioned in Corollary 3, we use the optima of this program in the first stage to infer the sparsity patterns of canonical directions. Also we can show that for every $(\gamma_{1j}, \gamma_{2j})$ that results in $\mathbf{z}_{1j}^* = 0$ according to the Corollary 3, there is a $\gamma'_{2j} \geq \gamma_{2j}$ in Program 10 for which $\mathbf{z}_{2ji}^* = 0$.

In the rest of this section we introduce *Block Sparse Multi-View CCA* and *Block Sparse Directed CCA*.

4.2 l_1 -Regularized Block Multi-View CCA

Now we extend our approach from 4.1 to identify correlation structures between more than two views, $\mathbf{X}_i \in \mathbb{R}^{n \times p_i}$, $i = 1, \dots, m$. The application of such methods are ever-increasing, e.g. understanding the enriched genetic pathways in a population of patients with a specific type of cancer. We extend the approach introduced in (Solari, Brown, and Bickel 2019) to our block setting, which results in the following optimization program,

$$\begin{aligned} \phi_{l_1,d}^m(\mathbf{\Gamma}_1, \dots, \mathbf{\Gamma}_d) = \max_{\substack{\mathbf{Z}_i \in \mathcal{S}_d^{p_i} \\ \forall i=1, \dots, m}} & \sum_{r < s=2}^m \operatorname{tr}(\mathbf{Z}_r^\top \mathbf{C}_{rs} \mathbf{Z}_s \mathbf{N}) \\ & - \sum_{j=1}^d \sum_{s=2}^m \sum_{\substack{r=1 \\ r \neq s}}^{s-1} \gamma_{srj} \|\mathbf{z}_{sj}\|_1 \end{aligned} \quad (11)$$

where $\mathbf{\Gamma}_j \in [0, 1]^{p_j \times M}$ are the sparsity parameter matrices whose elements γ_{srj} regulate the sparsity of canonical direction \mathbf{z}_{sj} in relation to \mathbf{z}_{rj} , where \mathbf{z}_{sj} is the j -th column of \mathbf{Z}_s . As before $\mathbf{C}_{rs} = 1/n \mathbf{X}_r^\top \mathbf{X}_s$ is a sample covariance matrix.

Theorem 5 Maximizers $\mathbf{Z}_i^*, i = 1, \dots, m$ of Program 11 are,

$$\begin{aligned} z_{sij}^*(\gamma_{sr1}, \dots, \gamma_{srd}) = & \operatorname{sgn} \left(\sum_{\substack{r=1 \\ r \neq s}}^m \tilde{\mathbf{c}}_{rsi}^\top \mathbf{z}_{rj} \right) [\mu_j \left| \sum_{\substack{r=1 \\ r \neq s}}^m \tilde{\mathbf{c}}_{rsi}^\top \mathbf{z}_{rj} \right| - \sum_{\substack{r=1 \\ r \neq s}}^m \gamma_{srj}]_+ \\ & \sqrt{\sum_{k=1}^{p_2} [\mu_j \left| \sum_{\substack{r=1 \\ r \neq s}}^m \tilde{\mathbf{c}}_{rsk}^\top \mathbf{z}_{rj} \right| - \sum_{\substack{r=1 \\ r \neq s}}^m \gamma_{srj}]_+^2} \end{aligned} \quad (12)$$

and for $r = 1, \dots, m$ and $r \neq s$,

$$\begin{aligned}
\mathbf{Z}_r^*(\boldsymbol{\Gamma}_1, \dots, \boldsymbol{\Gamma}_d) = & \\
\arg \max_{\substack{\mathbf{Z}_r \in \mathcal{S}_d^{pr} \\ r \neq s, r=1, \dots, m}} & \sum_{j=1}^d \sum_{i=1}^{p_s} [\mu_j | \sum_{\substack{r=1 \\ r \neq s}}^m \tilde{\mathbf{c}}_{rsi}^\top \mathbf{z}_{rj} | - \sum_{\substack{r=1 \\ r \neq s}}^m \gamma_{srj}]_+^2 + \\
\sum_{\substack{i < r = 2 \\ i, r \neq s}}^m & \text{tr}(\mathbf{Z}_i^\top \mathbf{C}_{ir} \mathbf{Z}_r \mathbf{N}) - \sum_{j=1}^d \sum_{\substack{i=1 \\ i \neq s}}^{p_s} \sum_{\substack{r=1 \\ r \neq s \\ i \neq j}}^{s-1} \gamma_{irj} \|\mathbf{z}_{ij}\|_1
\end{aligned} \tag{13}$$

Similar to the previous section, we drop the last term in Program 13 following the same justifications offered in Remark 4. This approximation leaves us with a concave minimization program which can be solved in a significantly faster and more stable way.

Corollary 6 *Given the sparsity parameter matrices $\boldsymbol{\Gamma}_i, i = 1, \dots, d$ and the solution, \mathbf{Z}_r^* for $r = 1, \dots, m$ and $r \neq s$, to the Equation 13,*

$$[\mathbf{T}_s]_{ij} = \begin{cases} 0 & |\sum_{\substack{r=1 \\ r \neq s}}^m \tilde{\mathbf{c}}_{rsi}^\top \mathbf{z}_{rj}| \leq 1/\mu_j \sum_{\substack{r=1 \\ r \neq s}}^m \gamma_{srj} \\ 1 & \text{otherwise} \end{cases} \tag{14}$$

4.3 l_1 -Regularized Directed CCA

Often samples involved in a multi-view learning problem are part of a designed experiment which differ along the direction of some treatment vector, or an observational study where we have information about the samples in addition to the observed views, e.g. socioeconomic status, sex, education level, etc. (Solari, Brown, and Bickel 2019) coined the term *Accessory Variable* to avoid confusions with the rich lexicon of statistical inference, to point out that this extra piece of information will be solely used to direct canonical directions such that they capture correlation structures which also align with these accessory variables, denoted here by $\mathbf{Y} \in \mathbb{R}^{n \times d}$, towards each column of which we direct the canonical directions. To this end, we form the following optimization problem,

$$\begin{aligned}
\phi_{l,d}(\boldsymbol{\gamma}_1, \boldsymbol{\gamma}_2, \boldsymbol{\epsilon}_1, \boldsymbol{\epsilon}_2) = & \max_{\substack{\mathbf{Z}_1 \in \mathcal{S}_d^{p_1} \\ \mathbf{Z}_2 \in \mathcal{S}_d^{p_2}}} \text{tr}(\mathbf{Z}_1^\top \mathbf{C}_{12} \mathbf{Z}_2 \mathbf{N}) \\
& - \sum_{i=1}^2 [\mathcal{L}(\mathbf{X}_i \mathbf{Z}_i \mathbf{N} \mathbf{E}_i, \mathbf{Y}) + \boldsymbol{\gamma}_i^\top \mathbf{l}(\mathbf{Z}_i)]
\end{aligned} \tag{15}$$

where $\mathbf{E}_i = \text{diag}(\boldsymbol{\epsilon}_i)$ are diagonal hyper-parameter matrices controlling the effect of the accessory variables on the canonical directions. $\mathcal{L}(\mathbf{A}, \mathbf{B}) : \mathcal{X}_A \times \mathcal{X}_B \rightarrow \mathbb{R}$ is a measure of column-wise misalignment of \mathbf{A} and \mathbf{B} . Here, we choose the Euclidean inner-product as our alignment measure, i.e. $\mathcal{L}(\mathbf{X}_i \mathbf{Z}_i \mathbf{N} \mathbf{E}_i, \mathbf{Y}) = -\langle \mathbf{X}_i \mathbf{Z}_i \mathbf{N} \mathbf{E}_i, \mathbf{Y} \rangle = -\text{tr}(\mathbf{Y}^\top \mathbf{X}_i \mathbf{Z}_i \mathbf{N} \mathbf{E}_i)$. Plugging in 15 and decoupling,

$$\begin{aligned}
\phi_{l_1,d}(\boldsymbol{\gamma}_1, \boldsymbol{\gamma}_2) = & \max_{\mathbf{Z}_1 \in \mathcal{S}_d^{p_1}} \sum_{j=1}^d \max_{\mathbf{z}_{2j} \in \mathcal{S}_d^{p_2}} [\mu_j \mathbf{z}_{1j}^\top \mathbf{C}_{12} \mathbf{z}_{2j} \\
& + (\mu_j \epsilon_{1j} \mathbf{y}_j^\top \mathbf{X}_2 \mathbf{z}_{2j} - \gamma_{2j} \|\mathbf{z}_{2j}\|_1)] \\
& + \sum_{j=1}^d (\mu_j \epsilon_{2j} \mathbf{y}_j^\top \mathbf{X}_1 \mathbf{z}_{1j} - \gamma_{1j} \|\mathbf{z}_{1j}\|_1) \tag{16}
\end{aligned}$$

where \mathbf{z}_{ij} is the j -th column of the i -th dataset.

Theorem 7 *Maximizers of Program 16 are,*

$$\begin{aligned}
\mathbf{Z}_1^* = \arg \max_{\mathbf{Z}_1 \in \mathcal{S}_d^{p_1}} & \sum_{j=1}^d \sum_{i=1}^{p_2} [\mu_j |\mathbf{c}_i^\top \mathbf{z}_{1j} + \epsilon_{2j} \mathbf{x}_{2i}^\top \mathbf{y}_j| - \gamma_{2j}]_+^2 \\
& + \sum_{j=1}^d (\mu_j \epsilon_{1j} \mathbf{y}_j^\top \mathbf{X}_1 \mathbf{z}_{1j} - \gamma_{1j} \|\mathbf{z}_{1j}\|_1) \tag{17}
\end{aligned}$$

and,

$$[\mathbf{Z}_2]_{ij}^* = \tag{19}$$

$$\begin{aligned}
& \frac{\text{sgn}(\mathbf{c}_i^\top \mathbf{z}_{1j} + \epsilon_{2j} \mathbf{x}_{2i}^\top \mathbf{y}_j) [\mu_j |\mathbf{c}_i^\top \mathbf{z}_{1j} + \epsilon_{2j} \mathbf{x}_{2i}^\top \mathbf{y}_j| - \gamma_{2j}]_+}{\sqrt{\sum_{k=1}^{p_2} [\mu_j |\mathbf{c}_k^\top \mathbf{z}_{1j} + \epsilon_{2j} \mathbf{x}_{2k}^\top \mathbf{y}_j| - \gamma_{2j}]_+^2}} \\
& \tag{20}
\end{aligned}$$

In the following corollary we formalize the necessary and sufficient conditions under which z_{2ij}^* is active using Equation 19.

Corollary 8 $[\mathbf{T}_2]_{ij} = 0$, iff $|\mathbf{c}_k^\top \mathbf{z}_{1j}^* + \epsilon_{2k} \mathbf{x}_{2k}^\top \mathbf{y}_j| \leq \gamma_{2j}/\mu_j$.

In the following section we propose algorithms to solve the optimization programs discussed so far.

Please refer to the *Supplements* for detailed proofs of the theorems and corollaries presented above as well as a discussion of l_0 -regularized Canonical Correlation Analysis.

5 BLOCCS: Gradient Ascent Algorithms for Regularized Block Models

As discussed so far, we reformulated each of the four cases studied into a concave minimization program over a Stiefel manifold. Our proposed algorithms involve a simple first-order optimization method at their cores, see *Supplements*. In 5.1 we apply this first-order method to the scenarios discussed so far, which constitutes the first stage of our two-stage approach. In the first stage, we estimate the sparsity patterns of our canonical directions. In the second stage we estimate the “active” entries (non-zero loadings) of the canonical directions using an alternating optimization algorithm discussed in 5.2.

5.1 Sparsity Pattern Estimation

In the first stage we estimate the sparsity patterns of the canonical directions, T_i , by applying each of the following algorithms once for each dataset. As we move from estimating T_1 to T_m , we use a technique which we term *Successive Shrinking*, that is having estimated T_i , we shrink every sample covariance matrix $C_{ij}, j \neq i$ to $[C'_{ij}]_{rs} = [C_{ij}]_{\tau_{ik}^{(r)} s}$,

where $\tau_{ik}^{(r)}$ is the r -th non-zero element of the k -th column of the i -th sparsity pattern matrix. As a result, in each successive shrinkage the covariance matrices are shrunk drastically, which in turn results in significant speed-up of our algorithm.

l_1 -Regularized Algorithm Now we apply our first-order maximization algorithm to Equation 10,

Algorithm 1: BLOCCS algorithm for solving Program 10

Data: Sample Covariance Matrix C_{12}
 Regularization parameter vector $\gamma_2 \in [0, 1]^d$
 Initialization $Z_1 \in \mathcal{S}_d^{p_1}$
 $N = \text{diag}(\mu_1, \dots, \mu_d) \succ 0$
 (optional) $T_1 \in \{0, 1\}^{p_1 \times d}$

Result: T_2 , optimal sparsity pattern of Z_2^*

1 initialization;
 2 while convergence criterion is not met do

3 for $j = 1, \dots, d$ do

4 $z_{1j} \leftarrow \sum_{i=1}^{p_2} \mu_j [\mu_j |c_i^\top z_{1j}| - \gamma_2] + \text{sgn}(c_i^\top z_{1j}) c_i$

5 $Z_1 \leftarrow \text{polar}(Z_1)$

6 if T_1 is given then

7 $Z_1 \leftarrow Z_1 \circ T_1$

8 Output $T_2 \in \{0, 1\}^{p_2 \times d}$ where $[T_2]_{ij} = 0$ if $|c_i^\top z_{1j}^*| \leq \gamma_2 / \mu_j$ and 1 otherwise.

As we pointed out above, we then compute T_1 using successive shrinkage.

Remark 9 One of the appealing qualities of our algorithm is that it is solely dependent on a function which can evaluate power iterations, which can be implemented very efficiently by exploiting sparse structures in the data matrix and canonical directions. This quality is significantly rewarded by successive shrinkage. It can also very easily be deployed on a distributed computing infrastructure. (S. Solari et al. 2019) utilize this quality to offer a Spark-based distributed regularized multi-view learning package.

Multi-View Block Sparse Algorithm We now propose an algorithm to solve Program 13, leaving out the regularization term in the first stage.

Directed Block Regularized Algorithm Before we present our algorithm, it is helpful to realize that the directed regularized case in Equation 16 is equivalent to the multi-modal case in Equation 11 with $m = 3$ and $\epsilon_i = \mathbf{1}_d$. As though we regard the accessory variable \mathbf{y} as a third view.

Algorithm 2: BLOCCS algorithm for solving Program 13

Data: Sample Covariance Matrices $C_{rs}, 1 \leq r < s \leq m$
 Sparsity parameter matrices $\Gamma_j \in [0, 1]^{m \times m}$ for $j = 1, \dots, d$
 Initial values $Z_r \in \mathcal{S}_r^{p_r}, 1 \leq r \leq m$
 $N = \text{diag}(\mu_1, \dots, \mu_d) \succ 0$
 (optional) $T_r \in \{0, 1\}^{p_r \times d}, r \neq s$

Result: T_s , optimal sparsity pattern for Z_s

1 initialization;
 2 while convergence criterion is not met do

3 for $r = 1, \dots, m, r \neq s$ do

4 for $j = 1, \dots, d$ do

5 $z_{rj} \leftarrow \sum_{i=1}^{p_r} \mu_j [\mu_j |c_{rsi}^\top z_{rj}| - \sum_{r \neq s}^m \gamma_{srj}] + \text{sgn}(\sum_{r \neq s}^m c_{rsi}^\top z_{rj}) c_{rsi} + \mu_j \sum_{l=1, l \neq r, s}^m \tilde{C}_{rl} z_{lj}$

6 $Z_r \leftarrow \text{polar}(Z_r)$

7 if T_r is given then

8 $Z_r \leftarrow Z_r \circ T_r$

9 Output $T_s \in \{0, 1\}^{p_s \times d}, [T_s]_{ij} = 0$ if $|\sum_{r \neq s}^m \tilde{C}_{rsi}^\top z_{rj}| \leq 1 / \mu_j \sum_{r \neq s}^m \gamma_{srj}$ and 1 otherwise.

But many times the researcher wants to have a direct control on how much effect the accessory variable will have on the canonical directions. Basically the larger ϵ_{ij} , the smaller the aperture of the convex cone that contains both \mathbf{y} and the canonical covariate $\mathbf{X}_i \mathbf{z}_i$. Below is the algorithm we devised for this problem,

In Section 6.2, we demonstrate the capabilities of this approach in exploratory data analysis and hypothesis development.

5.2 Active Entry Estimation

In the second stage of the algorithm, we estimate the active elements of the canonical directions for which, following (Journée et al. 2010), we also propose alternating algorithm to solve the following optimization program,

$$\phi_{d,0} = \max_{\substack{Z_1 \in \mathcal{S}_d^{p_1}, Z_1|_{\neq 0} = T_1 \\ Z_2 \in \mathcal{S}_d^{p_2}, Z_2|_{\neq 0} = T_2}} \text{tr}(Z_1^\top C_{12} Z_2 N) \quad (21)$$

Our simulations show that for small enough $\gamma_i, i = 1, 2$ such local maximizers exist.

The same algorithm is used in the multi-modal case by maximizing over a single Z_i while keeping others constant and looping over all canonical directions. In the directed case, we use the same ϵ_i we used in the first stage and it's again very similar to the multi-modal case. Although simple, we've included the corresponding algorithms for the two cases as well as algorithm for the l_0 -regularized CCA in the *Supplements*.

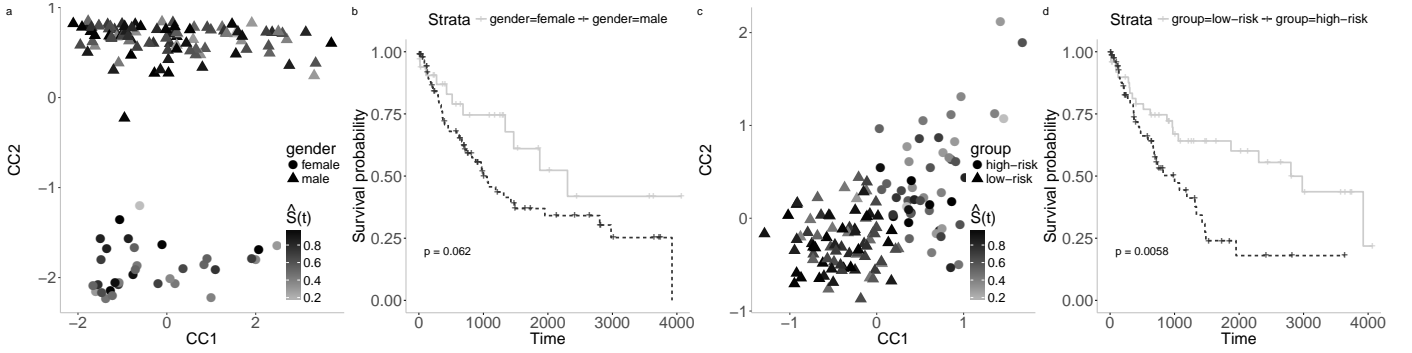


Figure 1: **a.** kmeans clustering of the samples projected onto the canonical directions estimated by applying *sCCA* to methylation and RNA-Seq datasets for LUSC patients, shape-coded by gender, and color-coded by $\hat{S}(t)$, i.e. the empirical survival distribution. **b.** $\hat{S}(t)$ for the two identified groups which precisely corresponded to gender rather than survival probability. **c.** kmeans clustering of the samples projected onto the canonical directions estimated by applying *Directed sCCA* to the same views and using $\hat{S}(t)$ as an accessory variable, color-coded by $\hat{S}(t)$. **d.** $\hat{S}(t)$ of the two identified groups by the *Directed sCCA* correspond to two significantly different, $p - value = 0.0058$, high-risk and low-risk survival groups.

Algorithm 3: BLOCSS algorithm for solving equation 16

Data: Sample Covariance Matrix C_{12}
 Regularization parameter vector $\gamma_2 \in [0, 1]^d$
 Hyper-parameter vectors $\epsilon_i \in \mathbb{R}^d, i = 1, 2$
 Initialization $Z_1 \in \mathcal{S}_d^{p_1}$
 $N = diag(\mu_1, \dots, \mu_d) \succ 0$
 (optional) $T_1 \in \{0, 1\}^{p_1 \times d}$

Result: T_2 , optimal sparsity pattern of Z_2^*

1 initialization;
 2 while convergence criterion is not met do
 3 for $j = 1, \dots, d$ do
 4 $z_{1j} \leftarrow \sum_{i=1}^{p_2} \mu_j [\mu_j |c_i^\top z_{1j} + \epsilon_{2j} x_{2i}^\top y| - \gamma_2] + sgn(c_i^\top z_{1j} + \epsilon_{2j} x_{2i}^\top y) c_i + \epsilon_{1j} X_1^\top y$
 5 $Z_1 \leftarrow polar(Z_1)$
 6 if T_1 is given then
 7 $Z_1 \leftarrow Z_1 \circ T_1$

8 Output $T_2 \in \{0, 1\}^{p_2 \times d}$ where $[T_2]_{ij} = 0$ if $|c_i^\top z_{1j}^* + \epsilon_{2j} x_{2i}^\top y| \leq \gamma_2 / \mu_j$ and 1 otherwise.

Algorithm 4: BLOCSS algorithm for solving equation 21

Data: Sample Covariance Matrix C_{12}
 Initialization $Z_i \in \mathcal{S}_d^{p_i}$ for $i = 1, 2$
 $N = diag(\mu_1, \dots, \mu_d) \succ 0$
 $T_i \in \{0, 1\}^{p_i \times d}$ for $i = 1, 2$

Result: $Z_i^*, i = 1, 2$, local maximizers of 21

1 initialization;
 2 while convergence criterion is not met do
 3 $Z_2 \rightarrow polar(C_{12}^\top Z_1 N) \circ T_2$
 4 $Z_1 \rightarrow polar(C_{12} Z_2 N) \circ T_1$

6 Experiments

In this section we first demonstrate performance characteristics of BLOCSS on simulated data; then we apply our approach to *Lung Squamous Cell Carcinoma(LUSC)* multi-omics from *The Cancer Genome Atlas*(Weinstein et al. 2013).

6.1 Simulated Data

Here we compare BLOCSS to PMA (Witten and Tibshirani 2009), which is a commonly used package and is a good representative of the approaches based on alternating optimization scheme which is the dominant school of approaches to the sCCA problem. We applied both methods to the pairs of views $\mathbf{X}_i, i = 1, 2$ estimate the first two pairs of canonical directions $\mathbf{Z}_i, i = 1, 2$, where $\mathbf{X}_i \sim \mathcal{N}(\mathbf{0}_{p_i}, \mathbf{C}_{ii}), i = 1, 2$, and $\mathbf{C}_{ii} = \mathbf{V}_i \mathbf{D} \mathbf{V}_i^\top$. We chose $p_1 = p_2, p_i/n = 10$, and constructed $\mathbf{V}_1 \in \mathbb{R}^{p_1 \times p_1}$ by setting up the first two columns as

$$\mathbf{v}_{11} = [\underbrace{1, \dots, 1}_{p_1/10}, 0, \dots, 0], \mathbf{v}_{12} = [\underbrace{0, \dots, 0}_{p_1/10}, \underbrace{1, \dots, 1}_{p_1/10}, 0, \dots, 0]$$

and the rest of the columns by sampling according to

$$[\mathbf{V}_{1j}]_{j=2}^{p_1} \sim \mathcal{N}(\mathbf{0}_{p_1-2}, \mathbf{I}_{p_1-2}).$$

Similarly, $\mathbf{V}_2 \in \mathbb{R}^{p_2 \times p_2}$,

$$\mathbf{v}_{21} = [0, \dots, 0, \underbrace{1, \dots, 1}_{p_2/10}], \mathbf{v}_{22} = [0, \dots, 0, \underbrace{1, \dots, 1}_{p_2/10}, \underbrace{0, \dots, 0}_{p_2/10}]$$

$$[\mathbf{V}_{2j}]_{j=2}^{p_2} \sim \mathcal{N}(\mathbf{0}_{p_2-2}, \mathbf{I}_{p_2-2})$$

We also set $\mathbf{D} = diag(\sigma_1, \sigma_2, \underbrace{\sigma, \dots, \sigma}_{p_1-2})$, where $\sigma_1/\sigma_2 = 2$, and $\sigma_3 = \dots = \sigma_{p_i} = \sigma$. We sampled \mathbf{X}_i for 100 different values of σ , repeated 10 times, each time computing

the average correlation of estimated canonical direction, z_{ij} and the underlying model, $z_{ij} = v_{ij}$ for $j = 1, 2$, see Figure 2.a and 2.b, and also the average correlation of the first and second estimated directions, see Figure 2.c, vs. the λ_3/λ_2 , where λ_i is the i -th eigenvalue of the sample covariance matrix, C_{12} . It is clear from Figure 2 that our approach learn the underlying model with superior accuracy while summarizing independent pieces of information in different canonical covariates. We guess that the apparent orthogonality of PMA estimates are mainly due to the fact that they contain minimal information about the underlying model.

6.2 TCGA: Lung Squamous Cell Carcinoma(LUSC)

We first performed sCCA between methylation and RNA-expression datasets obtained via TCGA2STAT(Wan, Allen, and Liu 2015). We used a permutation test, see Supplements, for hyper-parameter tuning. While the analysis provided in (Wan, Allen, and Liu 2015) filters out transcripts/CpG sites with expression/methylation level falling into the 99th percentile, we didn't filter out any covariates to simulate an fully automated pipeline. Despite this disadvantage, `bloccs` also identified two distinct clusters, with (between cluster distance)/(within cluster radius) = 9.79 compared to their 2.66, as plotted in Figure 1.a. However, contrary to their interpretation that these two groups indicate two different survival groups, as they point out the evidence against H_0 : *two survival distributions are the same* is weak; A Mantel-Cox test returns p – value = 0.062, $\chi^2_1 = 3.5$. We found out that the clusters precisely capture the `sex` effect rather than survival. We repeated the analysis, but this time we used our novel *Directed sCCA* method of Algorithm 3 with $\hat{S}(t)$ as the accessory variable. As a result we identified 25 genes and 44 CpG sites which are associated with each other and also associated with survival. Projecting the individuals onto the canonical directions, we identified two distinct clusters using kmeans clustering, see Figure 1.c. We then computed the Kaplan-Meier curves for these two groups separately in Figure 1.d. These two distributions are significantly different with p – value = 0.0058, $\chi^2_1 = 7.6$.

7 Conclusion

We presented a block sparse CCA algorithm suitable for very high-dimensional settings. The method we propose and the software we provide are more stable than previous implementations of sparse CCA. Of particular interest to us is the felicity of this method to incorporate a “guide vector” – or an experimental design, termed *accessory variables* in this article. In our lung cancer example, we included empirical survival distribution as an accessory variable, and explored genes and CpG sites that are associated with each other and patient survival probability. Indeed, we find the tuning parameters of our algorithm useful tools for data exploration, enabling the user to view a variety of relationships between views correlated more or less with an accessory variable. While multi-omics studies in biology were the motivation behind creating `bloccs`, we anticipate utility in a number of domains within and beyond the biomedical sciences.

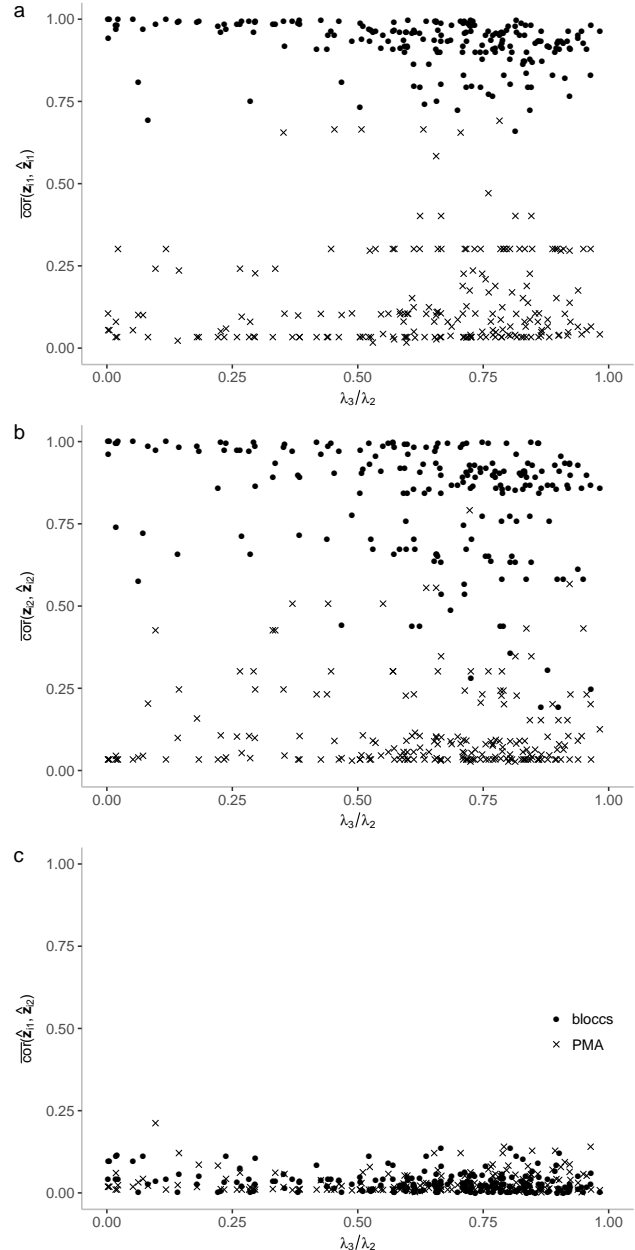


Figure 2: **a,b.** The average correlation of the “true”, underlying model, and estimated first, and second respectively, pair of canonical directions. **c.** Average within pair correlation of the estimated directions. (plotted points are running medians).

References

Andrew, G.; Arora, R.; Bilmes, J.; and Livescu, K. 2013. Deep canonical correlation analysis. *International Conference on Machine Learning* 1247–1255.

Blaschko, M. B.; Shelton, J. A.; Bartels, A.; Lampert, C. H.; and Gretton, A. 2011. Semi-supervised kernel canonical correlation analysis with application to human fmri. *Pattern Recognition Letters* 32(11):1572–1583.

Chaudhary, K.; Poirion, O. B.; Lu, L.; and Garmire, L. X. 2018. Deep learning-based multi-omics integration robustly predicts survival in liver cancer. *Clinical Cancer Research* 24(6):1248–1259.

Chu D., Liao L., N. M. K. Z. X. 2013. Sparse canonical correlation analysis: New formulation and algorithm. *IEEE TRANSACTIONS ON PATTERN ANALYSIS AND MACHINE INTELLIGENCE* 35.

Hopkins, C. 1969. Statistical analysis by canonical correlation: a computer application. *Health services research* 4(4):304.

Hotelling, H. 1935. The most predictable criterion. *Journal of Educational Psychology* 26:139–142.

Huang, H.; He, H.; Fan, X.; and Zhang, J. 2010. Super-resolution of human face image using canonical correlation analysis. *Pattern Recognition* 43(7):2532–2543.

Journée, M.; Nesterov, Y.; Richtrárik, P.; and Sepulchre, R. 2010. Generalized power method for sparse principal component analysis. *Journal of Machine Learning Research* 11:517–553.

Lai, P., and Fyfe, C. 2000. Kernel and nonlinear canonical correlation analysis. *International Journal of Neural Systems* 10:365–377.

Li, Y.; Wu, F.-X.; and Ngom, A. 2016. A review on machine learning principles for multi-view biological data integration. *Briefings in bioinformatics* 19(2):325–340.

Monmonier, M., and Finn, F. 1973. Improving the interpretation of geographical canonical correlation models. *The Professional Geographer* 25:140–142.

Parkhomenko, E.; Tritchler, D.; and Beyene, J. 2009. Sparse canonical correlation analysis with application to genomic data integration. *Statistical Applications in Genetics and Molecular Biology* 8:1–34.

S. Solari, O.; P. Duncan, J.; Safavi, R.; B. Brown, J.; and J. Bickel, P. 2019. Sparkle: A generalized spark-based sparse kernel multi-view learning framework. *arXiv preprint arXiv:1206.3242*.

Simonson, D.; Stowe, J.; and Watson, C. 1983. A canonical correlation analysis of commercial bank asset/liability structures. *Journal of Financial and Quantitative Analysis* 10:125–140.

Solari, O. S.; Brown, J. B.; and Bickel, P. J. 2019. Sparse canonical correlation analysis via concave minimization. *arXiv preprint arXiv*.

Tu, X.; Burdick, D.; Millican, D.; and McGown, L. 1989. Canonical correlation technique for rank estimation of excitation-emission matrices. *Analytical Chemistry* 19(61):2219–2224.

Waaijenborg, S.; Verselewel de Witt Hamer, P.; and Zwinderman, A. 2008. Quantifying the association between gene expressions and dna-markers by penalized canonical correlation analysis. *Statistical Applications in Genetics and Molecular Biology* 7.

Wan, Y.-W.; Allen, G. I.; and Liu, Z. 2015. Tcgab2stat: simple tcga data access for integrated statistical analysis in r. *Bioinformatics* 32(6):952–954.

Weinstein, J. N.; Collisson, E. A.; Mills, G. B.; Shaw, K. R. M.; Ozenberger, B. A.; Ellrott, K.; Shmulevich, I.; Sander, C.; Stuart, J. M.; Network, C. G. A. R.; et al. 2013. The cancer genome atlas pan-cancer analysis project. *Nature genetics* 45(10):1113.

Witten, D., and Tibshirani, R. 2009. Extensions of sparse canonical correlation analysis with applications to genomic data. *Statistical Applications in Genomics and Molecular Biology* 8.

Wong, K.; Fung, P.; and Lau, C. 1980. Study of the mathematical approximations made in the basis correlation method and those made in the canonical-transformation method for an interacting bose gas. *Physical Review* 3(22):1272.